processes

MDPI

Article

Base-Level Fluctuation Controls on Migration of Delta Lobes: A Case Study from the Paleogene Shahejie Formation in the Huimin Depression, Bohai Bay Basin, NE China

Renchao Yang [1,2,3,*], Yang Li [3], Xuepeng Wu [4,*], Jianqiang Di [3], Junjian Zhang [3] and Nils Lenhardt [5]

[1] State Key Laboratory of Shale Oil and Gas Enrichment Mechanisms and Effective Development, Beijing 102206, China
[2] Laboratory for Marine Mineral Resources, Qingdao National Laboratory for Marine Science and Technology, Qingdao 266071, China
[3] College of Earth Science and Engineering, Shandong University of Science and Technology, Qingdao 266590, China
[4] Research Institute of Petroleum Engineering, SINOPEC, Beijing 102206, China
[5] Department of Geology, University of Pretoria, Private Bag X20, Pretoria 0028, South Africa
* Correspondence: r.yang@sdust.edu.cn (R.Y.); wuxp.sripe@sinopec.com (X.W.)

Abstract: Sandbody distribution patterns and controls are the most important foundation for petroleum exploration and development, particularly in a lacustrine basin with rapid changes in the sedimentary environment. To provide sedimentologists and petroleum geologists around the world with an analogue for sandstone reservoir prediction, the sedimentary facies of the fourth member of the Shahejie Formation (Sha-4 Member) in the Huimin Depression of the Bohai Bay Basin were analyzed, and the sequence stratigraphic framework was established based on characteristics of spontaneous potential logs and lithology. According to the findings of this study, the Sha-4 Member's sedimentary environment was dominated by delta front and shallow lake facies. Delta front sandbodies were discovered to retrograde before prograding again throughout the established profile. The Sha-4 Member in the Huimin Depression is divided into a third-order sequence (LSC1), which can be further divided into four fourth-order sequences (MSC1 to MSC4), corresponding to the four sub-members (S4-1 to S4-4). During the development of the MSC1 to MSC4 sequences, the delta depositional scale first decreased and then increased with the changing base level. The maximum flooding surface developed within the MSC3 sequence. The Sha-4 Member sequence model reveals that the deltas in the study area exhibit self-similarity, and delta sandbodies are primarily developed in the MSC1, MSC2, and MSC4, whereas mudstone is largely developed in the MSC3.

Keywords: base level fluctuations; sequence stratigraphy; lacustrine deltas; Huimin Depression; Paleogene

Citation: Yang, R.; Li, Y.; Wu, X.; Di, J.; Zhang, J.; Lenhardt, N. Base-Level Fluctuation Controls on Migration of Delta Lobes: A Case Study from the Paleogene Shahejie Formation in the Huimin Depression, Bohai Bay Basin, NE China. *Processes* **2023**, *11*, 378. https://doi.org/10.3390/pr11020378

Academic Editor: Qingbang Meng

Received: 13 December 2022
Revised: 17 January 2023
Accepted: 22 January 2023
Published: 25 January 2023

1. Introduction

Modern high-resolution sequence stratigraphy is a useful method to determine sedimentary facies migration and reservoir distribution in many oil-bearing basins around the world [1–10]. A change in the base level affects the sediment supply and accommodation space, consequently influencing the degree of sediment preservation, stratigraphic accumulation style, and thus, facies types and sequences. However, these base level cycles are mostly based on sea level fluctuations [11–23]. Research on base level cycles based on lake level changes, for instance, in fault basins, is much less well-known and remains underrepresented in the literature on sequence stratigraphy [24–26].

The Bohai Bay Basin in northeast China is a Mesozoic to Cenozoic fault basin that is dominated by the Huimin Depression. The 4th member (Sha-4 Member) of the Paleogene Shahejie Formation within the Huimin Depression has been shown to have a good oil and

gas play, most notably in the Linxie 108 well drilled in the study area. As a result, the Sha-4 Member is expected to have significant exploration and development potential in this area. A variety of publications on the general sedimentology and reservoir characterization of the Huimin Depression have already been released [27–35]. Nevertheless, despite these efforts, an understanding of the Sha-4 Member's stratigraphic sequence remains relatively weak and cannot meet current exploration needs, as a clear understanding of the stratigraphic sequence is a key factor in the further development of oil and gas fields.

The present contribution primarily investigates the controls of base level cycles on the delta lobes within the depression in order to provide a reference for the prediction of favorable reservoirs in the Sha-4 Member and to further the exploration and development of the oil fields within the Huimin Depression. This is accomplished by combining the sequence stratigraphic characteristics of the Sha-4 Member with the distribution characteristics of delta sandbodies. The said approach may also be employed to forecast sandstone reservoirs in lacustrine deltas influenced by lake level fluctuations in other faulted basins around the world.

2. Geological Setting

The Huimin Depression is located in the northwest of the Shandong Province in eastern China. The depression extends axially in the northeast direction, with a length of about 130 km from east to west, a width of about 35–70 km from north to south, and an area of 7000 m^2 [36]. It is closely connected with the Dongying Depression in the east, the Linqing Depression in the west, the Luxi High in the south, and the Chengning High in the north.

The study area is located in the central and western regions of the Huimin Depression. It is bordered to the north by the Zizhen Depression, to the south by the Linnan Depression, and to the east and west by the Linyi Fault branches. The sedimentary succession of the Huimin Depression comprises Jurassic to Quaternary deposits (Figure 1). The Paleogene Shahejie Formation can be subdivided into four different members, Sha-1 Member (Es_1) to Sha-4 Member (Es_4), that are numbered in descending order. The Sha-4 Member is the main focus of this contribution and can be further divided into Sha-4 lower and Sha-4 upper sub-members. The lithology of the lower sub-member of Es_4 is dominated by gray mudstone, mixed with dark red siltstone and conglomerate. The lithology of the upper sub-member of Es_4 is mainly characterized by the interbedding of grayish brown and dark gray sandstones and dark mudstones. Blackish brown oil shale, containing small amounts of carbonaceous shale, may also occur.

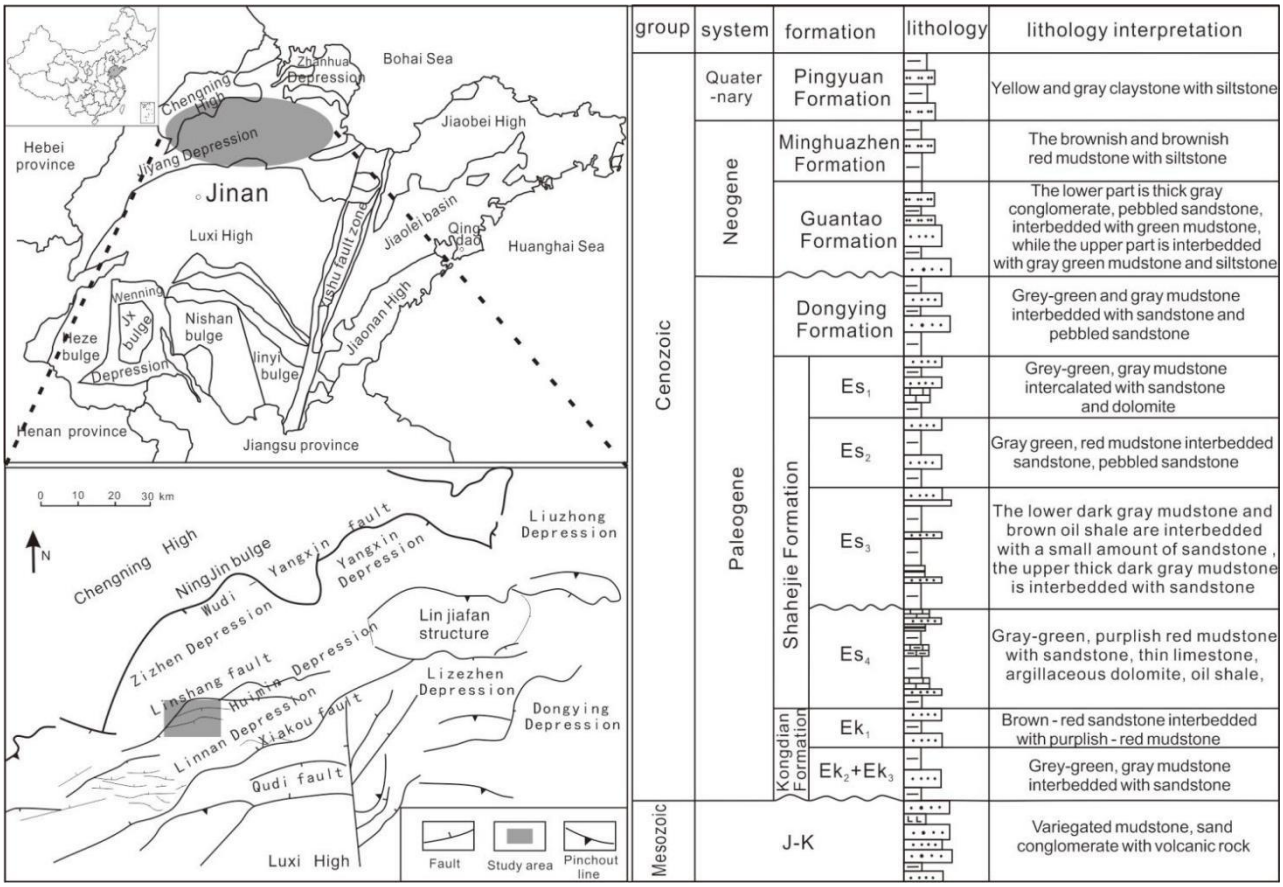

Figure 1. Huimin Depression structure map (**left**) and stratigraphy of the Huimin Depression (**right**).

3. Data and Methods

A sedimentary facies analysis of the Sha-4 Member was carried out, and a sequence stratigraphy was established based on 183 wells distributed within the Linxie 108 Block in the study area (for clarity, only 54 wells appear in the maps), in order to characterize the influence of base level cycles on the distribution of different sedimentary facies and, in particular, for hydrocarbon exploration.

This paper mainly applies the spontaneous logs. Since the spontaneous potential (SP) is generated by the diffusion and adsorption of ions in rocks, which are closely related to rock properties (rock composition, texture, composition, cement, etc.), the lithology can be analyzed using changes in the SP curve [37,38]. The mudstone is represented by the baseline on the spontaneous potential curve, while the sandstone is reflected by negative anomalies. Thus, lithologies of mudstones and sandstones can be distinguished from each other by negative or positive deflection from the shale base line by measuring the sand content in the Sha-4 Member of the Shahejie Formation.

The purpose of this contribution is to provide a sandstone thickness isopach map of each sub-member in the study area based on the statistics of sandstone thickness data for each sub-member in the Sha-4 Member of 54 wells, combined with stratigraphic characteristics data. As the provenance is in the northwest of the depression [14], the sandstone thickness gradually decreases from the northwest to the southeast. Additionally, a plane distribution map of the sedimentary facies of the Sha-4 Member is provided. Within this article, the term "sand ratio" refers to the ratio of the total thickness of sandstone to the formation thickness. The direction of the sand ratio indicates the direction of the material source. The analysis of sedimentary facies through the sand-land ratio isopach map is one of the important research methods of sedimentology. We divided the study area into three sections: shore shallow lakes with a sand-land ratio of less than 0.3; delta front with a

sand-land ratio greater than 0.3 but less than 0.6; and delta plain with a sand-land ratio greater than 0.6.

To certify detailed sedimentary facies analysis via logs, a 26.5 m-core from Well L57 was examined based on colors, lithology, sedimentary structures, and trace fossils within these cores.

4. Results

4.1. Base Level Fluctuations

The identification and division of base level cycles are based on a combination of the characteristics of sedimentary facies and facies sequence changes [39]. The stratigraphic base level is not a completely fixed interface. In the process of change, it always shows a trend of unidirectional movement to the maximum or minimum amplitude of the base level, forming a complete base level rise and fall cycle. This rising and falling cycle of the base level is called the base level cycle [7]. The cyclicity of the sedimentation patterns within the Sha-4 Member is relatively apparent. The top interface of the Sha-4 Member is determined according to lithofacies and spontaneous potential characteristics data. Combined with the division of provenance direction and sedimentary facies, the Sha-4 Member is divided into one long-term cyclic sequence (LSC1) that can further be subdivided from top to bottom into four sand units: S4-1, S4-2, S4-3, and S4-4 (Figure 2). These four sand units correspond to four medium-term cycle sequences, which are MSC4, MSC3, MSC2, and MSC1, from top to bottom.

4.1.1. Long Term Cyclic Sequence

The long-term datum surface, which corresponds to the maximum flooding surface, is the sedimentary interface where the base level rises to the highest point and the water body is the deepest, and it is primarily controlled by relative sea level rise, tectonic factors, and climate [40]. The "long-term base level cycle" refers to the process of rising and falling of the regional base level within the sedimentary basin [7]. Using Well p61 as an example (Figure 2), the lithostratigraphy of the well shows an incomplete symmetrical long-term cycle with a deepening, followed by a shallowing upward. It is composed of incomplete symmetrical and nearly complete symmetrical medium-term cycles dominated by ascending semi-cycles, reflecting the continuous lacustrine transgression retrogradation sedimentary process in the study area.

4.1.2. Medium Cycle Sequence

In high-resolution sequence stratigraphy, the isochronous correlation of medium-term cyclic sequences is the most significant. The middle cycle sequence is a set of rock assemblages that share a common sedimentary background and genesis. It is formed by the superposition of many short-term cycles and shows obvious characteristics on the logging curve. It is typically the logging facies' conversion surface or catastrophe surface, which reflects the progradation and retrogradation assemblages of similar or adjacent facies sequences in the same sedimentary system [41].

The lithostratigraphy of Well p61, for instance, is divided into one long-term base level cycle and four medium-term base level cycles (Figure 2). Among them, MSC1 is an asymmetric type dominated by an ascending semi-cycle, which corresponds primarily to S4-1. The base level was in the early stages of rising when the lake level was low. At this time, the study area mainly developed a fan delta front, an underwater distributary channel was developed, water flow energy was strong, and sediment particle sizes were coarse. MSC2 is also an incomplete symmetrical type, dominated by an upwelling half cycle, which corresponds to S4-2. During this time, the lake level continued to rise, and the lake transgression increased, primarily along the delta front. MSC3 is an incomplete symmetrical type of descending and ascending semi-cycles. As illustrated in Figure 2, the base level rises first and then falls in this cycle, primarily corresponding to S4-3. The deposition of channel sandbodies was weakened during this period, and the grain sizes

of the sediments were fine, with mudstone and siltstone being the dominant lithologies. Finally, MSC4 is an incomplete symmetrical type that is dominated by a downward half cycle. At this time, the sediment particle size became coarser than before, and medium sandstone can be seen.

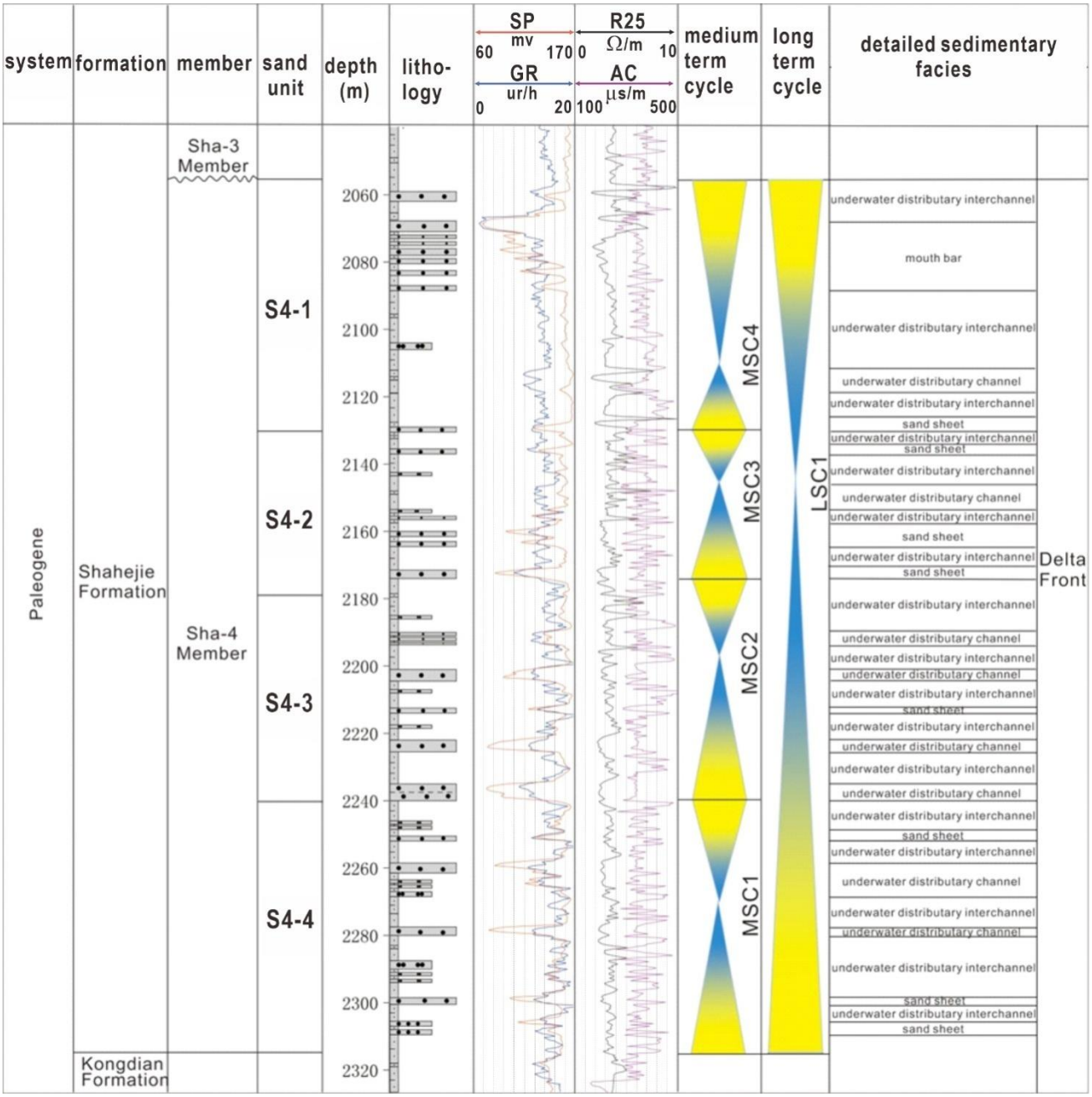

Figure 2. Comprehensive histogram of Well p61.

4.2. Sedimentary Facies Analysis

Based on observations and descriptions of drill cores from Well L57, combined with lithologic characteristics, logging data, and sedimentary facies markers such as lithology, grain sizes, and sedimentary structures, different sedimentary facies types, such as delta and shore-shallow lake, could be identified within the Sha-4 Member of the study area.

4.2.1. Sedimentary Facies Marker Analysis

The facies and microfacies in different sedimentary environments have different sedimentary characteristics, which can be identified by means of the corresponding facies markers. Sedimentary structure is an important index for distinguishing different sedimentary facies types [42]. The Sha-4 Member within the Huimin Depression is primarily characterized by a lithologic assemblage ranging from mudstones to fine-grained conglomerates and some minor carbonate rocks (Figure 3). Sedimentary structures include bedding and deformation features.

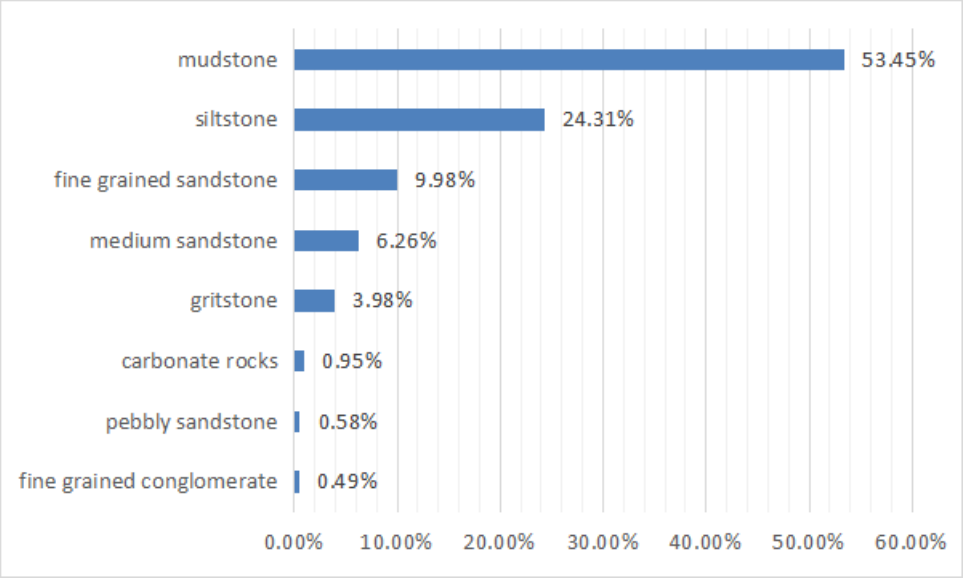

Figure 3. Lithology distribution of the Sha-4 Member.

The most common bedding structures in the study area are flow sand bedding, trough cross-bedding, and parallel bedding (Figure 4). Trough cross-bedding is most common in the lower reaches of a river channel, with the scale gradually increasing upstream. This bedding is mostly found in medium- and fine-grained sandstone (about 16.24%), which may also contain mud clasts. It forms in sedimentary environments, such as a distributary channel. Sand bedding is mostly formed by ripples on the sediment surface, which form in relatively calm, shallow waters. Scouring surfaces indicate a significant change in fluid velocity, indicating that hydrodynamic action was very active. These surfaces are frequently seen at the bottom of distributary channels. Deformation structures, formed by gravity-induced flow deformation of slope sediments, are mostly found in siltstone (about 24.31%). The Sha-4 Member's biogenic structures are predominantly traces of biological activities and biological growth structures. The biogenic structures differ greatly due to the different morphologies and living environments of different organisms. The study area contains structures such as biological disturbances and plant fossils.

Similar to sedimentary structure markers, logging facies markers are an important means of determining sedimentary facies type. Sedimentary facies can be identified more systematically using logging data response characteristics (curve amplitude, upper and lower contact relationships, smoothness, etc.) and core description and analysis [43].

Within the measured wells of the study area, box, bell, funnel, finger, and zigzag curves can be found (Figure 4). The smooth box curve lithology is dominated by sandstone of varying thicknesses (approximately 45.11%). An argillaceous interlayer exists in the corresponding sandbody. The toothed box curve's lithology is primarily sandstone, with an argillaceous interlayer in the corresponding sandbody. This curved shape frequently denotes sedimentary facies, such as an underwater distributary channel and a mouth bar. The bell curve shows that it gradually changes into mudstone as the mud content in sandstone increases. The logging curve is shaped like a bell, with high values at the

bottom and low values at the top. These curves mostly represent distributary channels. The opposite of the bell-shaped curve is the funnel-shaped curve. The lithology of the funnel-shaped curve is primarily sandstone, with the top of the sandbody in abrupt contact and the base in gradational contact with mudstone, indicating a mouth bar. Sandstone is the most common lithology of the finger-shaped curve. Its thickness is typically less than 2 m. The sand sheet is distinguished by its abrupt top and bottom contact with the mudstone. The micro-toothed curve has medium and low amplitude and is shaped like a tooth. The curve is generally close to the mudstone baseline. Its lithology is primarily mudstone (approximately 53.45%), representing interchannel bay and shallow lake shore facies.

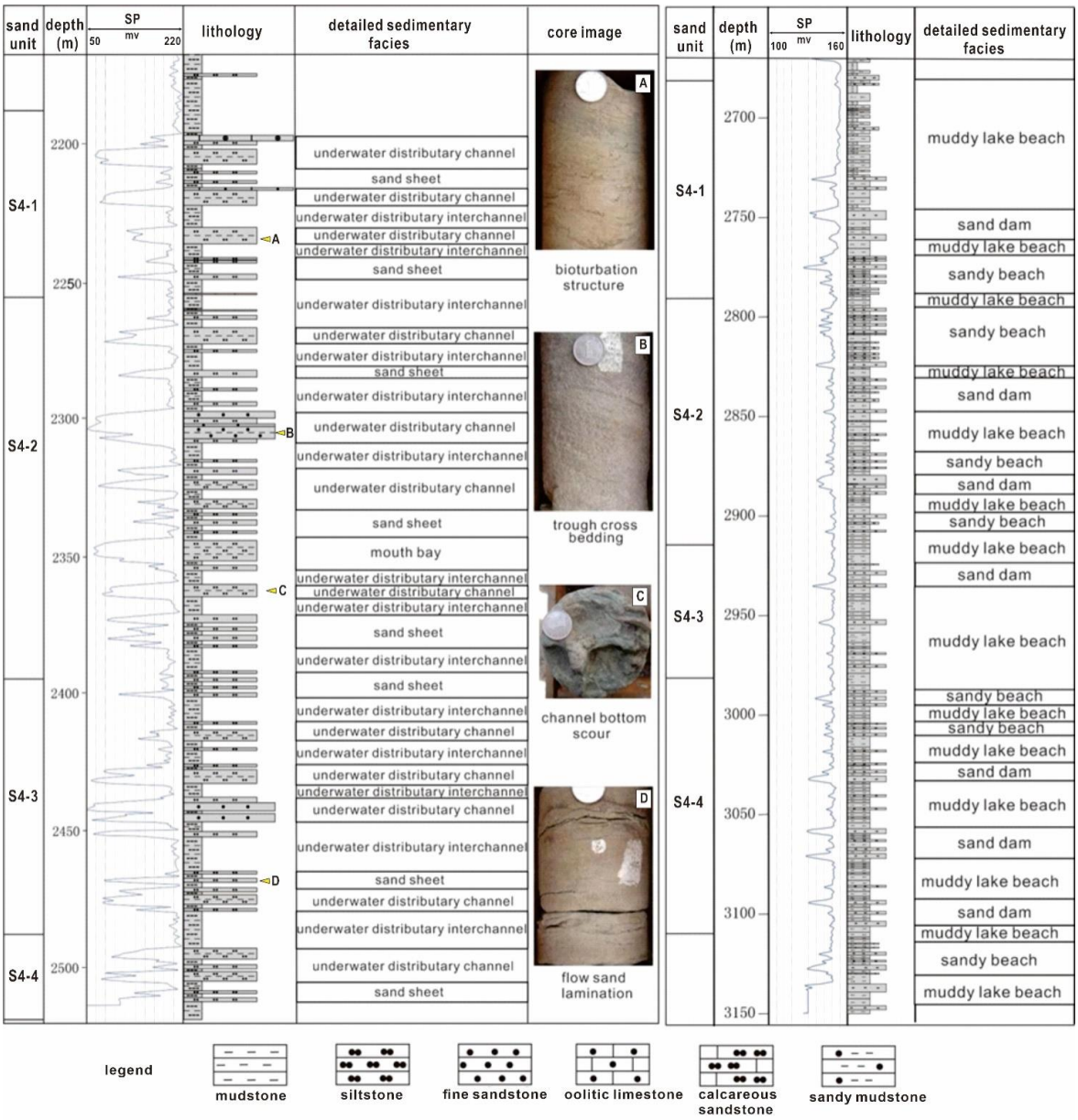

Figure 4. Delta front deposits of Well L57 (**left**) and shore shallow lake deposits of Well L202 (**right**). (**A**) bioturbation, 2235.03 m; (**B**) trough cross-bedding, 2305.42 m; (**C**) erosional scour, 2362.24 m; (**D**) flow sand lamination, 2468.08 m.

4.2.2. Sedimentary Structures

The core collected from Well L57 is characterized by the presence of four sand units (S4-1 to S4-4). Sand unit S4-1 is distinguished by light gray muddy siltstone with gray mud flasers. The flasers are interrupted by siltstone (Figure 4A). S4-2 is mostly made up

of light gray, medium-grained sandstone with curved mud flasers that have varying dip angles (Figure 4B). Additional siltstone appears rutted and uneven. At the base of one of the siltstones, erosional scour is present (Figure 4C). The presence of parallel mud flasers (Figure 4D) defines the S4-3 sand unit, which is mostly light gray siltstone.

The light gray muddy siltstone and interrupted mud flasers (Figure 4A) are interpreted as bioturbation. This, along with the other fine-grained sediments, paints a picture of an environment characterized by severe bioturbation and rapid deposition rates, with existing organisms possibly attempting to avoid being covered by the sediments. The corresponding depositional environment may have been the edge of an underwater distributary channel. The light gray medium-grained sandstone with curved mud flasers is interpreted as trough cross-bedding (Figure 4B). Trough cross-bedding is commonly formed by the migration of sand dunes within a strong hydrodynamic environment, such as an underwater distributary channel. The erosional scour (Figure 4C) is interpreted as the lowermost part of an underwater distributary channel. The light gray siltstone with parallel mud flasers (Figure 4D) is thought to be a flow sand lamination within a sand sheet. As a result, we can conclude that the sedimentary rocks of Well L57 primarily formed in a delta front environment.

4.2.3. Sedimentary Architectural Elements

Based on the above description and analysis of sedimentary facies markers and previous research results, it can be considered that the Sha-4 Member along the northwest provenance direction is primarily characterized by delta front and shore shallow lake deposition, with the delta front possibly having the widest extension (Figure 4). The delta front can be further divided into four architectural elements: underwater distributary channel, sand sheet, underwater distributary interchannel, and mouth bar. The feeding river is thought to have carried large amounts of sand and mud debris.

The distributary channel gradually advanced and eventually extended into the lake basin to form an underwater distributary channel. With further extension of the channel, the river gradually widened and increased its ability to branch out while the flow velocity started to slow down, gradually accumulating sediment. The lithology of this architectural element is mainly siltstone and fine sandstone, with a logging curve showing bell and box characteristics of medium and high amplitude. Existing sedimentary structures are frequently formed by cross-bedding, scours, deformation structures, and so on.

The mouth bar is a sandy sedimentary body that formed when the river entered the lake basin due to the sudden widening of the lake, which resulted in a decrease in flow velocity. Its lithology is mainly made up of sandstone. The spontaneous potential curve is funnel shaped. Sedimentary structures are commonly cross-bedding, ripple marks, etc.

The underwater distributary interchannel was formed in the low-lying lake bay area at the lower reaches of the river, with weak hydrodynamic conditions. The lithology is mainly mudstone, containing a small amount of dark fine clasts, such as fine sandstone and siltstone. Horizontal bedding is the dominant sedimentary structure. Furthermore, plant debris and other fossils may be seen. The spontaneous potential curve shows low-amplitude sawtooth or peak characteristics.

The sand sheet was formed by the lateral migration of the mouth bar. The thin sandbody is distributed in the form of a band. The lithology is mainly composed of fine sandstone, siltstone, and argillaceous siltstone. The spontaneous potential curve shows a finger shape of medium and high amplitude.

The shore shallow lake (Figure 4) element commonly formed in low-lying, flat terrain, with a concentration of rivers and waterways and a large water area. Beach bars (sandy lake beaches and sand bars) and muddy lake beaches are subsets of this element. Their sediment is mainly sourced from the nearby delta. The beach bar sedimentary system is developed in a place with sufficient debris supply, gentle terrain, and stable wave and current action. In contrast, the sandy lake beach in the study area was formed at the outer edge of the flat delta. Here, the lithology is characterized by the combination of

interbedded lakeside mudstone, siltstone, and sandy mudstone. The single-layer sandstone is thin, generally less than 1.5 m thick, with a symmetrical rhythmic structure, gradual contact of mud and sand, common wavy bedding in sedimentary structure, and a finger or knife-shaped logging curve.

The sand bar was formed within a shallow lake environment. In this environment, the depth of the water body is greater than that of the sandy lake beach. The hydrodynamic environment is strong. The lithology of this element is mainly siltstone, calcareous siltstone, and argillaceous siltstone, mixed with thinly layered mudstone. The sandbody is generally thick, composed of multiple cycles, mostly superimposed in the inverse rhythm of fine, coarse, and fine symmetry. Wavy bedding, cross-bedding, and other bedding structures are developed, as are mud and gravel slump deformation and other structures. The logging curve is characterized by a box or funnel shape. The argillaceous lake beach was formed within a flat terrain, a shallow water body, and a quiet hydrodynamic force. The lithologic types are mudstone and sandy mudstone with horizontal bedding. There are also traces of fossil fragments, such as plant roots and leaves. The curve shows a low-amplitude sawtooth shape near the shale baseline.

4.3. Profile Distribution Characteristics

According to the previous analysis of Section 4.1, the sedimentation of the Sha-4 Member was controlled by a long-term base level cycle that first deepened and then shallowed upward. Each sand unit is divided into one medium-term cycle, with a total of four medium-term cycle sequences, which can be seen in Figure 5. During the deposition of MSC1 (sand group 1 of Sha-4 Member), the sandbody as a whole was well developed. Similarly, during the deposition of MSC2 (sand group 2 of Sha-4 Member), the sandbody was also well developed, with more medium-thick sandbodies than that of MSC1, interspersed with some thin sandbodies and a smaller sandbody scale. During the deposition of MSC3 (sand group 3 of Sha-4 Member), the sandbody was also well developed, but the extension was generally short, and the continuity was poor. During the depositional period of MSC4 (sand group 4 of Sha-4 Member), thick sandbodies were developed in the north with good continuity. Here, the scale of the sandbodies is larger than that during the MSC3 sedimentary period.

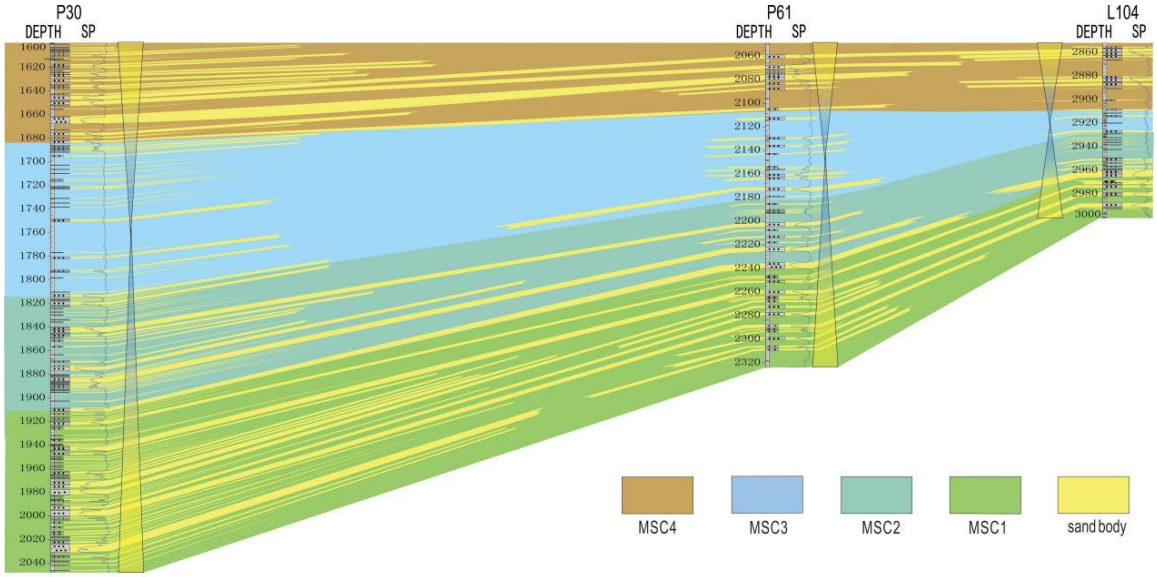

Figure 5. North-South well correlation of the Sha-4 Member in the study area.

In the east-west P32-P7 well correlation (cross-section) (Figure 6), the characteristics of sandbody development from MSC1 to MSC4 are similar to the north-south well correlation. Sandbodies developed during MSC1 decreased in size during MSC2. Dur-

ing the deposition of MSC3, the sandbody continuity was the lowest and the extension was generally the shortest. MSC4's thick sandbodies were primarily formed in the west, while the thinner sandbodies can be found in the east, with good continuity and extensive sandbody extension.

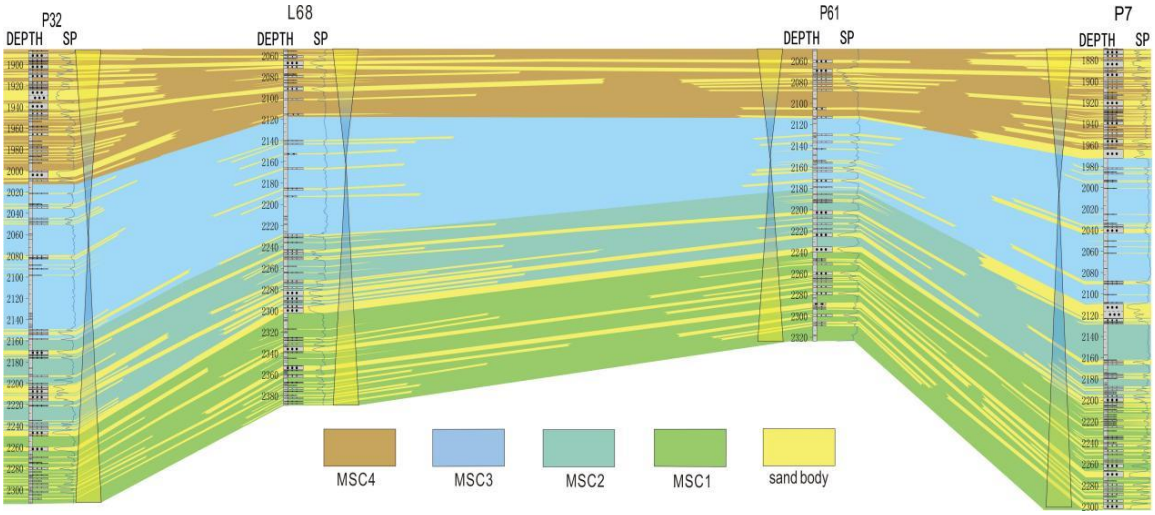

Figure 6. East-West well correlation of the Sha-4 Member in the study area.

4.4. Sandbody Distribution Characteristics

Based on the sandstone thickness data of each sand unit of the Sha-4 Member, several sandstone thickness isopach maps can be drawn for each sedimentary period of the member (Figures 7–10). Vertically, the area of sedimentary sandbodies first decreases and then expands from northwest to southeast from MSC1 to MSC4, owing to the depression's provenance to the north and northwest. Laterally, the thick sandbodies are mostly found in the northwest, close to the provenance. The sedimentary sand layers in the east and south are thinner. At the same time, the shore-shallow lake area in the northeast is dominated by beach bar deposits. Here, the cumulative thickness of sandstone is less than 10 m. In consequence, the shore-shallow lake area does not develop a large-scale, high-quality reservoir sandbody.

The MSC1 sedimentary period exhibits a large accommodation space, different sandbody thickness distributions, and a small distribution range of sedimentary sandbodies, indicating that it belongs to the early stages of delta development. The sedimentary environment of the underwater distributary channels is most widely distributed, and the sand thickness is generally high, exceeding 50 m (Figure 7). The accommodation space increased during MSC2 deposition, and the sandbody thickness was moderate. In the northwest provenance area, the sandbody was relatively well developed and had good continuity. In the area where sand sheets developed, the sandbody thickness is relatively thin. The shore-shallow lake area in the northeast is dominated by beach bars with low sandstone content and sand thicknesses of less than 10 m (Figure 8). During the deposition of MSC3, the base level and accommodation space increased, and the thickness of sandbodies in the study area decreased. During this period, a delta front environment dominated the study area (Figure 9). During the deposition of MSC4, the accommodation space was further reduced while the base level dropped to the lowest point of the Sha-4 Member. Nevertheless, areas with thick sandbodies were widely distributed within the study area. Under the influence of sediment supply, the delta front area prograded toward the southeast. The shore-shallow lake facies gradually declined, and the extent of the sedimentary sandbody reached its maximum within the Sha-4 Member, with thicknesses up to more than 60 m and generally around 50 m. The distributary channel area is dominated by sandstone, whereas the underwater distributary interchannel area is dominated by argillaceous sediments with generally undeveloped sandstone (Figure 10).

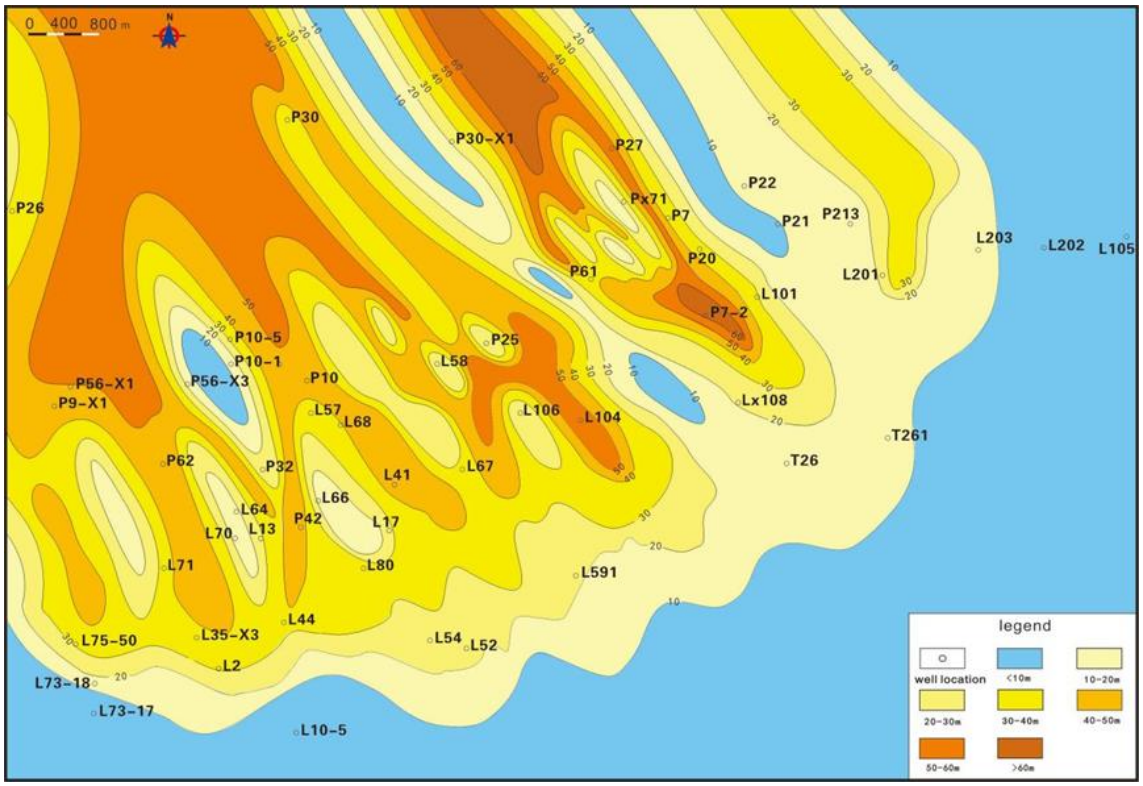

Figure 7. Isopach map of sandstone unit during the MSC1 period of the Sha-4 Member in the Huimin Depression.

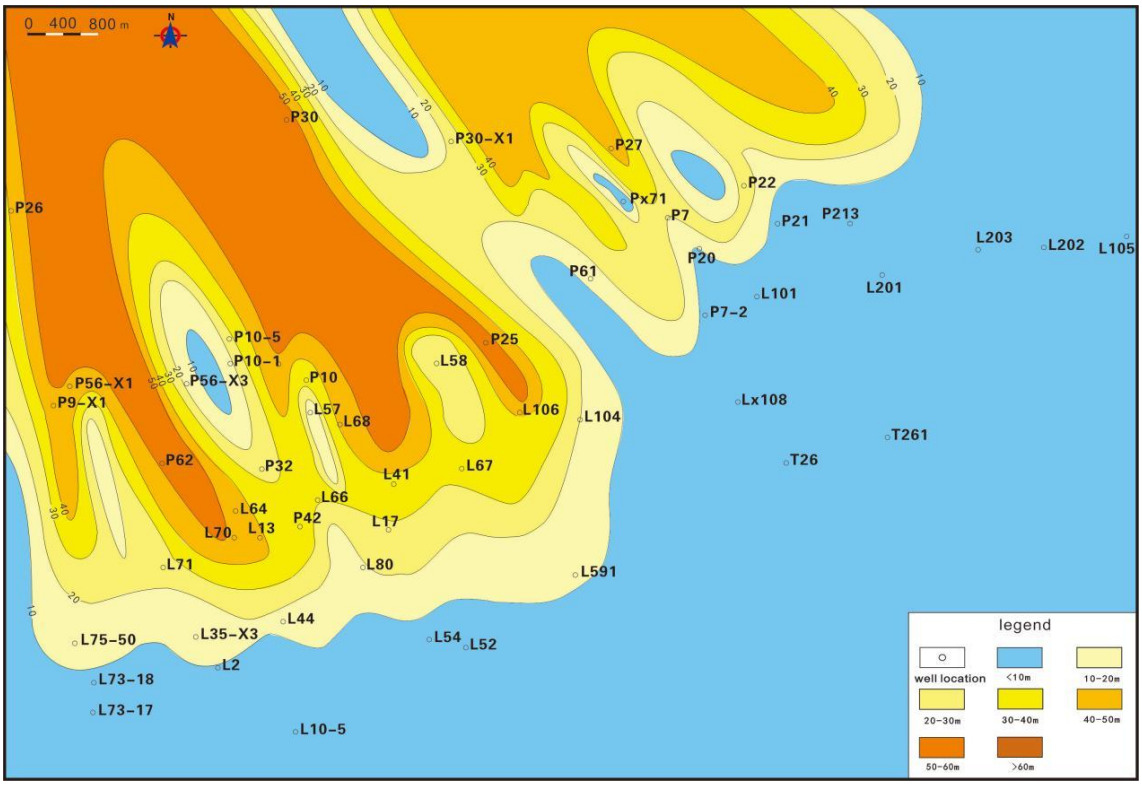

Figure 8. Isopach map of sand unit during the MSC2 period of the Sha-4 Member in the Huimin Depression.

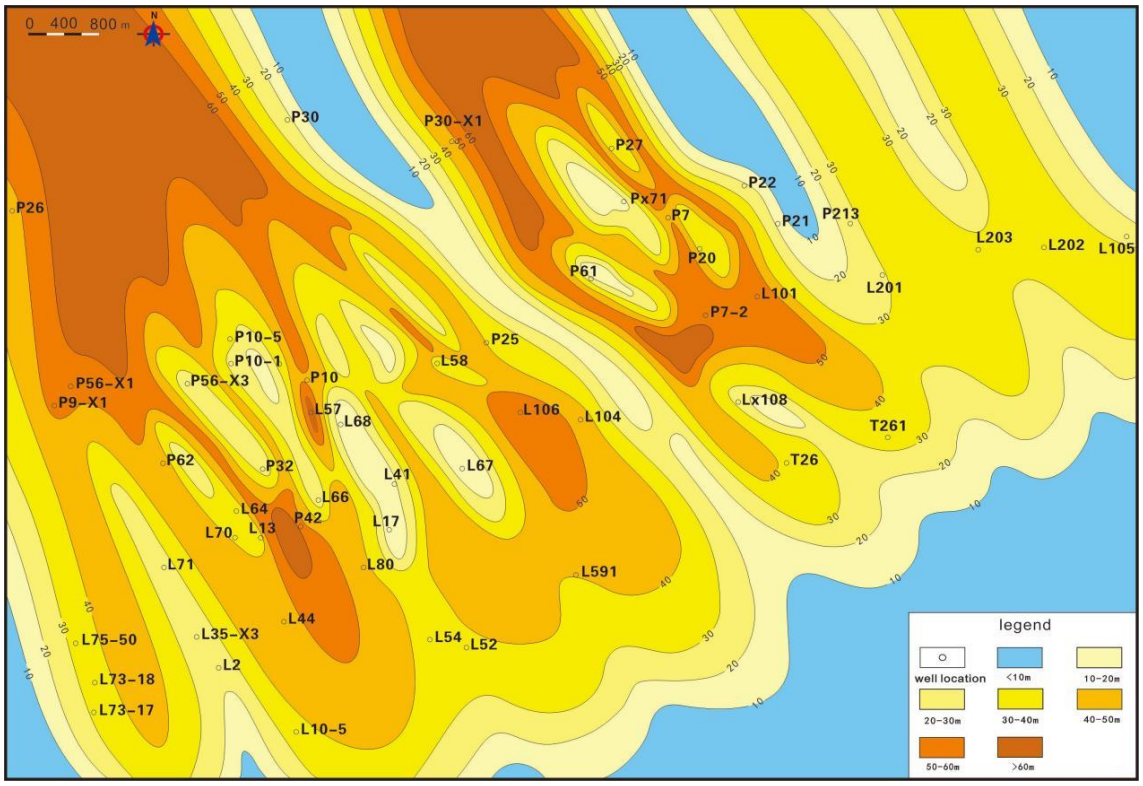

Figure 9. Isopach map of sand unit during the MSC3 period of the Sha-4 Member in the Huimin Depression.

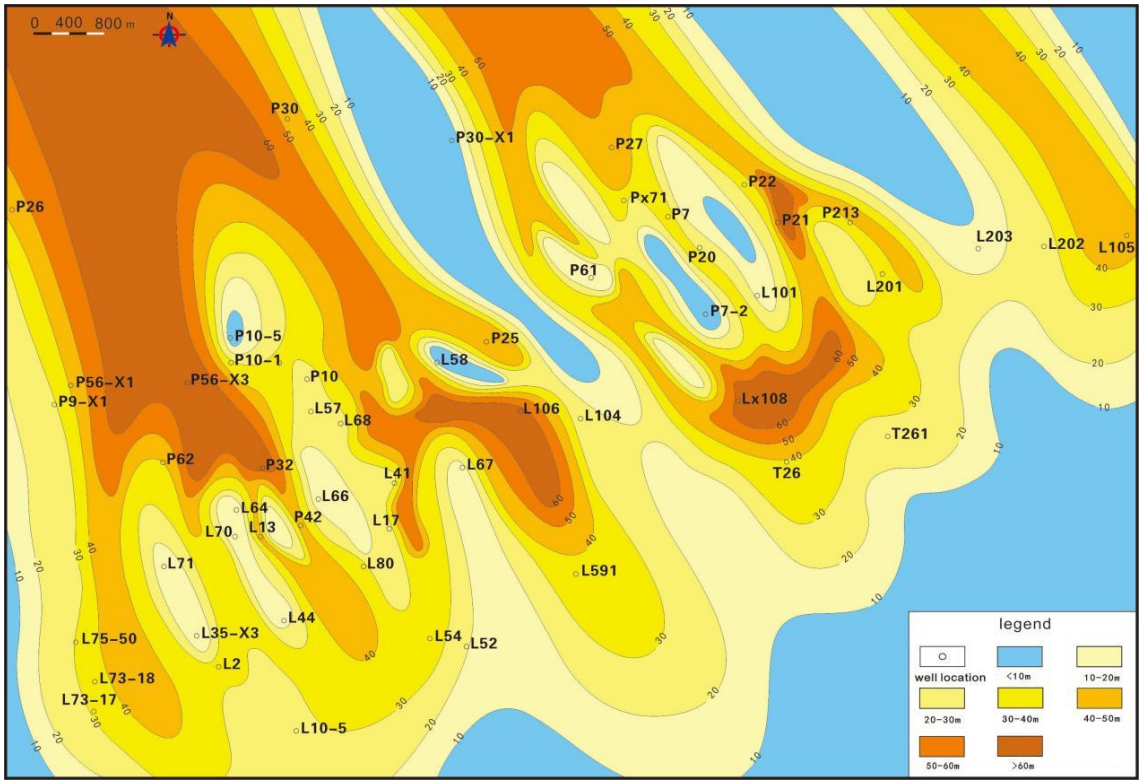

Figure 10. Isopach map of sand unit during the MSC4 period of the Sha-4 Member in the Huimin Depression.

5. Discussion

5.1. Plane Distribution Characteristics

According to the facies map (Figure 11), the MSC1 deposition is mainly characterized by retrogradation, and the sedimentary facies are primarily related to underwater distributary channels. The delta area was relatively small during the initial stage of deposition, while the lake area was relatively large. The delta front area in the study area was beginning to shrink at the time of MSC2 deposition, as was the delta plain facies belt (Figure 12). As a result, the river channel narrowed, and the lake grew rapidly. During the sedimentation period of MSC3, the delta facies first narrowed and then extended to the southeast lake (Figure 13). The delta area grew larger over time, and the range of shore-shallow lake facies shrank. During the MSC4 period, the delta facies began to expand, while the shore-shallow lake facies belt shrank further (Figure 14). The delta front occupied the majority of the study area, and the delta plain facies belt gradually migrated eastward. Simultaneously, the hydrodynamic conditions became stronger, resulting in the continuous interaction and superposition of sandbodies in the delta front.

5.2. Sequence Sand Control Model

Based on the study on the distribution characteristics of the delta sedimentary system in the Huimin Depression, combined with the sequence stratigraphic development model and temporal and spatial distribution characteristics of the study area, the sand control model of the delta sequence in the Sha-4 Member of the Huimin Depression is proposed from the aspects of accommodation space change rate and sedimentation rate (Figure 15).

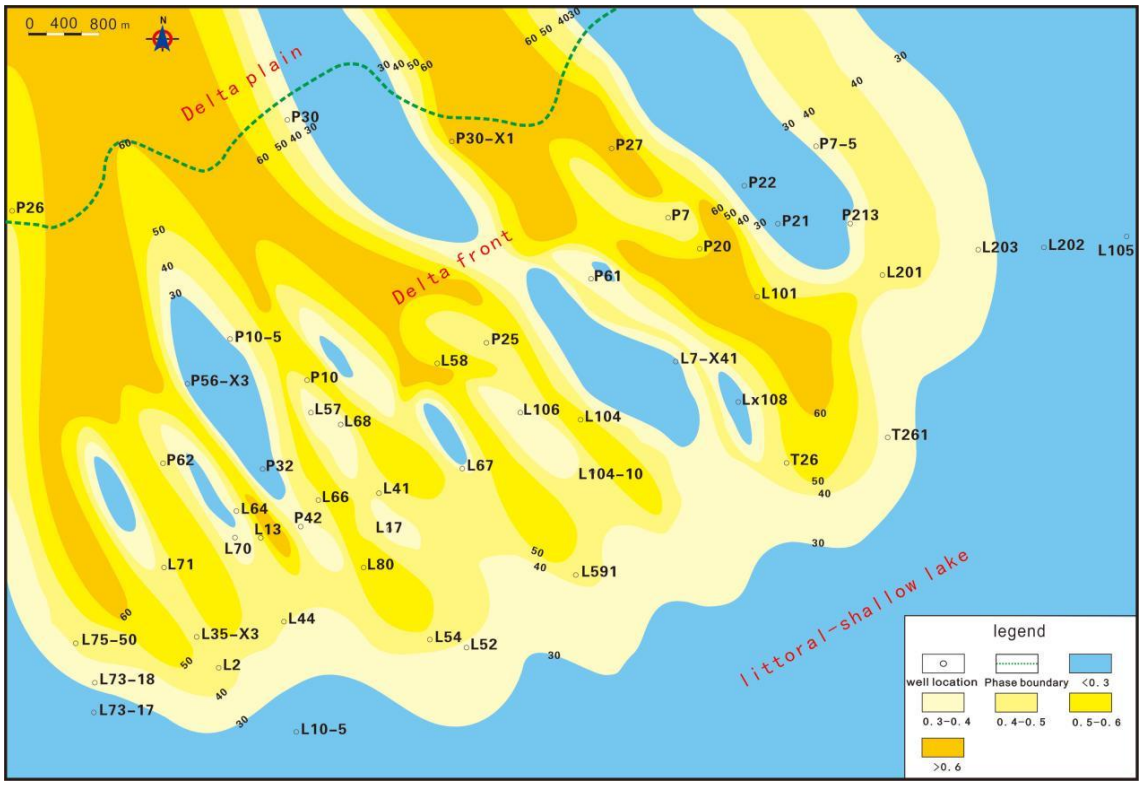

Figure 11. Sedimentary facies map during the MSC1 period of the Sha-4 Member in the Huimin Depression.

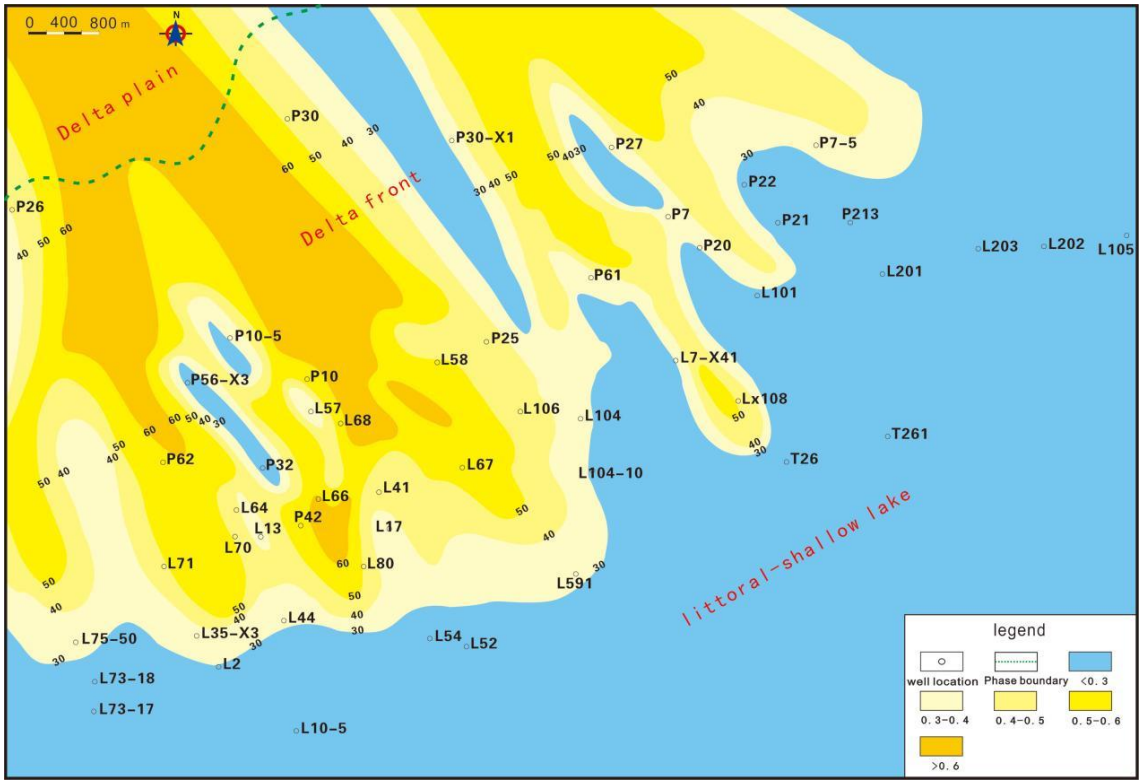

Figure 12. Sedimentary facies map during the MSC2 period of the Sha-4 Member in the Huimin Depression.

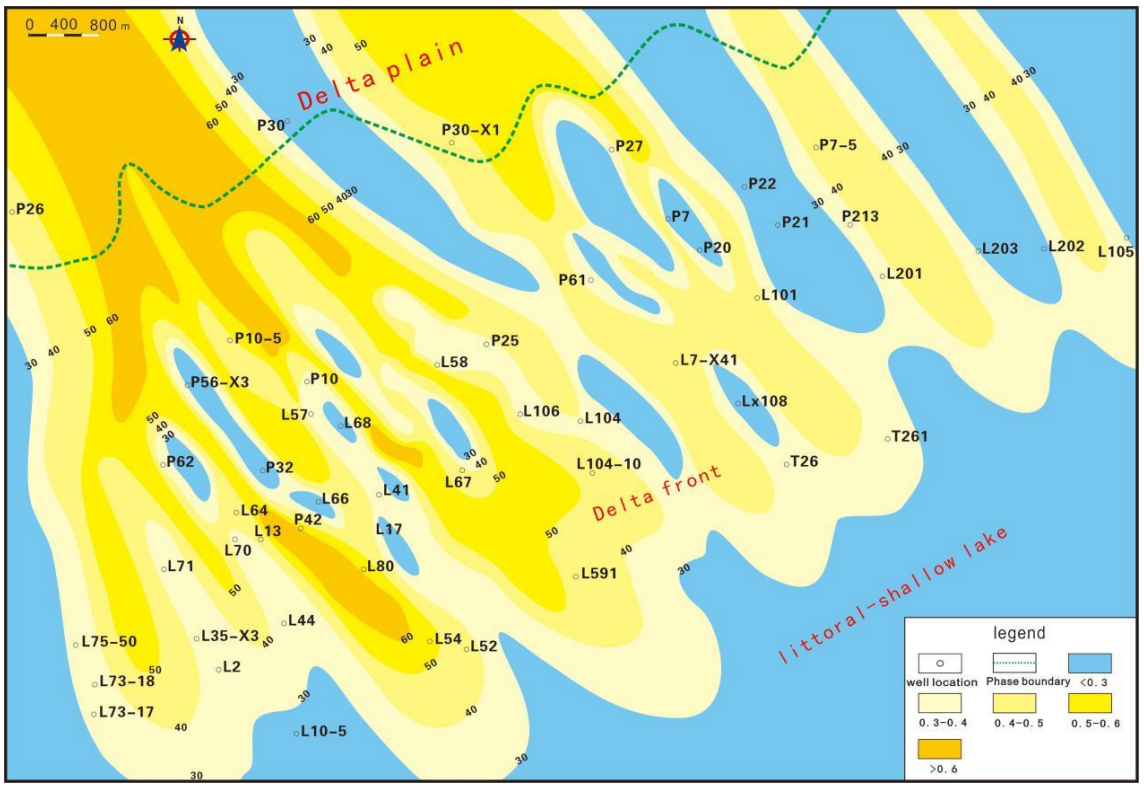

Figure 13. Sedimentary facies map during the MSC3 period of the Sha-4 Member in the Huimin Depression.

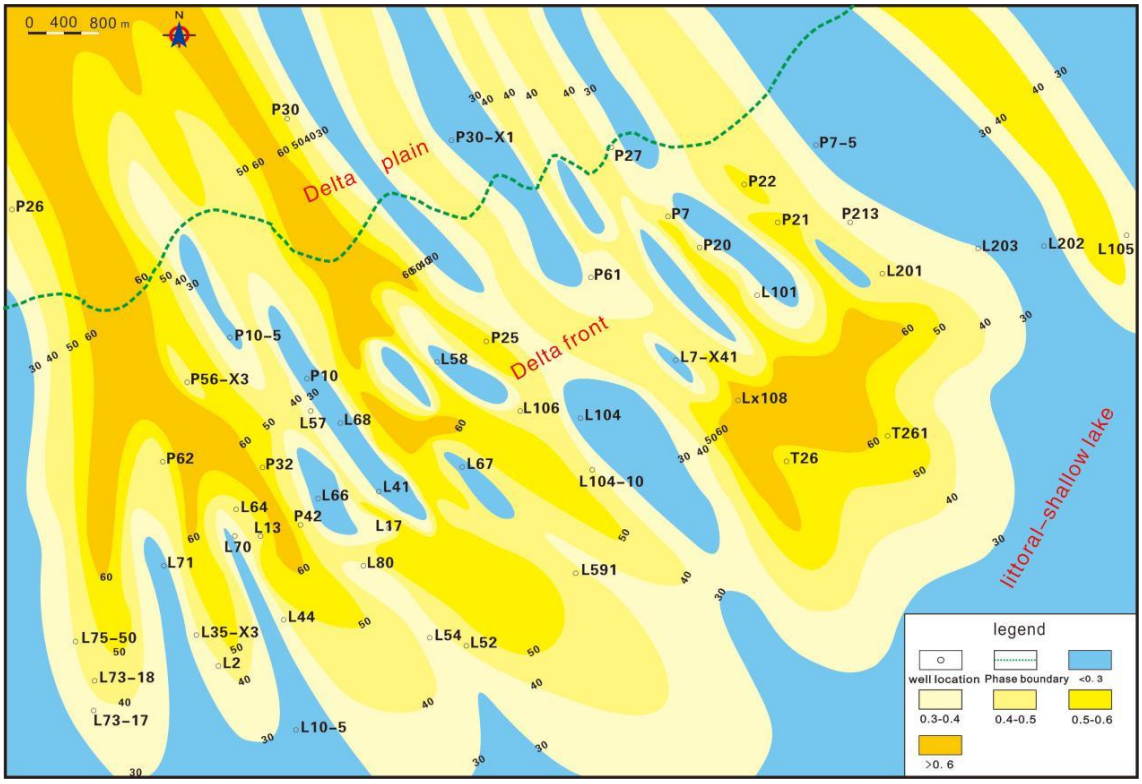

Figure 14. Sedimentary facies map during the MSC4 period of the Sha-4 Member in the Huimin Depression.

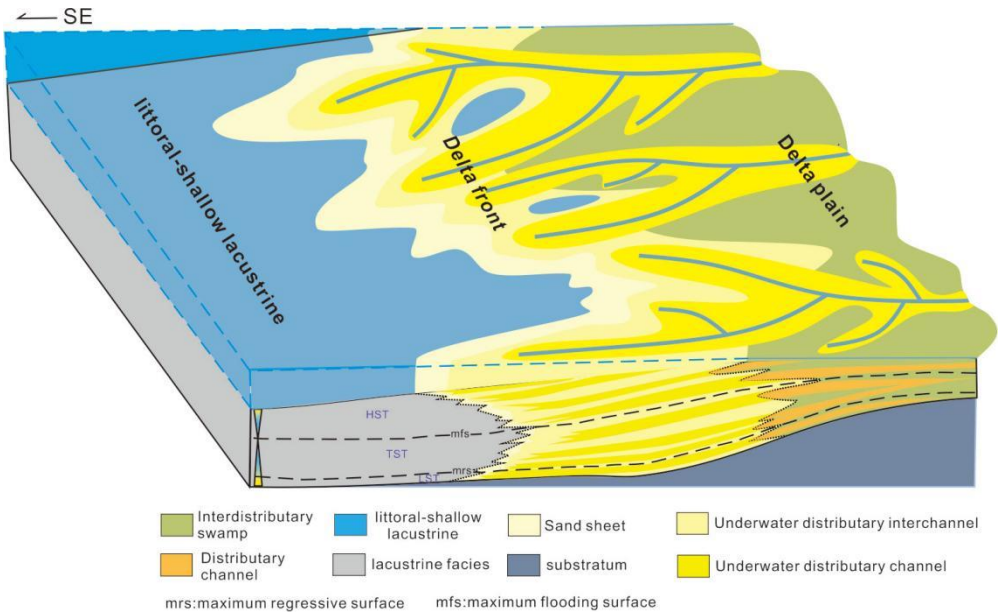

Figure 15. Block diagram of the depositional sequences of the Sha-4 Member.

This paper illustrates the sequence sand control model of the Sha-4 Member in the Huimin Depression using a third-order sequence as an example. The third-order sequence (long-term base level cycle) of the Sha-4 Member MSC1 and MSC2 was in the rising stage, and the change rate of accommodation space was greater than that of sediment supply, resulting in lake transgression. The sandbody continued to regress to the land, and the sedimentary trend gradually moved toward the shoreline. The MSC3 period, which is the transition period between the rise and fall of the base level cycle, has the

largest lake flooding surface of the third-order sequence. MSC4 was in the decline stage of the base level cycle in the third-order sequence, and the change rate of accommodation space was less than that of sediment supply, resulting in lake regression. The sandbody continued to accumulate towards the lake basin, and the sedimentary trend gradually moved towards the lake basin. According to sandbody distribution characteristics, Sha-4 Member sandbodies in the Huimin Depression are found primarily in MSC1, MSC2, and MSC4. Furthermore, different levels of cycles are known to have self-similarity in cycle symmetry and phase combination [44]. MSC1 and MSC2 are not completely symmetrical in the two middle-term cycles (fourth-order cycles), which are dominated by the rising base level semi-cycle. The MSC3 period cycle is a relatively complete symmetrical cycle. The MSC4 cycle is not completely symmetrical as the lower base level ascending interval (semi-cycle) is less developed than the upper base level descending interval (semi-cycle).

Sandbody formation may be influenced by factors such as sediment supply, tectonic activity, and paleogeomorphology. The sandstone within the study area generally formed when there was an abundance of coarse sediments. Tectonic activity may provide lodging space as well as a supply of sediment. Tectonic activity, erosion, and sediment deposition, in turn, have an impact on the basin's paleogeomorphology. Although sediment supply, tectonic activity, paleogeomorphology, and lake level fluctuations all have an impact on the sedimentary environment, the base level cycles are the result of the interaction of all these factors.

6. Conclusions

1. One long-term base level cycle (LSC1) and four medium-term base level cycles (MSC1-MSC4) are identified in the Sha-4 Member within the Huimin Depression. The long-term base level cycle generally conforms to the sedimentary process of lake transgression retrogradation. The medium-term base level cycle MSC1 corresponds to the fourth sand member of Es4, MSC2 corresponds to the third sand member of Es4, MSC3 corresponds to the second sand member of Es4, and MSC4 corresponds to the first sand member of Es4. The four medium-term cycles formed within a delta front environment.
2. The control of the base level cycles on the delta lobes is mainly reflected in the control of the delta front sandbody distribution. The lateral extent of sandbodies decreased and increased with the rise and fall of the base level, respectively.
3. Based on the distribution characteristics of sedimentary systems and sequence stratigraphy in the study area, a depositional model is proposed to illustrate the control of base level fluctuations on sandbody development and distribution. Deltaic sandbodies were mainly developed in MSC1, MSC2, and MSC4. Mudstone is mainly developed in MSC3.

Author Contributions: R.Y., project fund recipient, draft construction; Y.L., partial English written; X.W., data collection and draft construction; J.D., figure drawing and partial English written; J.Z., data processing; N.L., English Polishing and scientific moderation. All authors have read and agreed to the published version of the manuscript.

Funding: This study is financial supported by the Open Fund of State Key Laboratory of Shale Oil and Gas Enrichment Mechanisms and Effective Development (Grant Number: 33550000-22-ZC0613-0003) and the National Natural Science Fund of China (Grant Number: 41972146).

Data Availability Statement: Not applicable.

Acknowledgments: Anonymous reviewers and editors proposed constructive comments and suggestions, We are grateful to Shengli Oilfield Company for providing well and core data.

Conflicts of Interest: The authors declare no conflict of interest.

References

1. Cross, T.A. *Controls on Coal Distribution in Transgressive-Regressive Cycles, Upper Cretaceous, Western Interior, USA*; SEPM, Special Publication: Broken Arrow, OK, USA, 1998; Volume 42, pp. 371–380.
2. Cross, T.A. High-resolution stratigraphic correlation from the perspective of base-level cycles and sediment accommodation. *Proc. Northwestern Eur. Seq. Stratigr. Congr.* **1994**, 105–123.
3. Cross, T.A.; Lessenger, M.A. Sediment volume partitioning: Ratio-nale for stratigraphic model evaluation and high-resolution stratigraphic correlation. *Nor. Pet.-Foren. Conf.* **1996**, 1–24.
4. Xu, H.D. Several problems in the application of sequence stratigraphy theory to the analysis of faulted basins in China. *Oil Gas Geol.* **1997**, *18*, 83–89. (In Chinese with English abstract)
5. Deng, H.W.; Wang, H.L.; Ning, N. Principle of sediment volume distribution: Theoretical basis of high-resolution sequence stratigraphy. *Earth Sci. Front.* **2000**, *7*, 305–313. (In Chinese with English abstract)
6. Deng, H.W.; Wang, H.L.; Zhu, Y.J. *High Resolution Sequence Stratigraphy Principle and Application*; Geological Publishing House: Beijing, China, 2002; pp. 3–22. (In Chinese)
7. Zhu, X.M. *Sequence Stratigraphy*; Petroleum University Press: Dongying, China, 2000; pp. 147–156. (In Chinese)
8. Huang, Y.; Yao, G.; Fan, X. Sedimentary characteristics of shallow-marine fans of the Huangliu Formation in the Yinggehai Basin, China. *Mar. Pet. Geol.* **2019**, *110*, 403–419. [CrossRef]
9. Li, Y.; Yang, R.C. Astronomical calibration of a ten-million-year Triassic lacustrine record in the Ordos Basin, North China. *Sedimentology* **2022**, *70*, 407–433. [CrossRef]
10. Wu, J.; Liang, C.; Yang, R.C.; Xie, J. Sequence stratigraphic control on the variations of organic matter in Eocene lacustrine shales within the Dongying Depression, Eastern China. *J. Asian Earth Sci.* **2022**, *237*, 105353. [CrossRef]
11. Jean, B.P.; Andre, S. Platform-to-basin correlation by high-resolution sequence stratigraphy and cyclostratigraphy (Berriasian, Switzerland and France). *Sedimentology* **1997**, *44*, 1071–1092.
12. Gareth, T.G. Characterisation and high resolution sequence stratigraphy of storm-dominated braid delta and shoreface sequences from the Basal Grit Group (Namurian) of the South Wales Variscan peripheral foreland basin. *Mar. Pet. Geol.* **2000**, *17*, 445–475.
13. Gonzalo, D.V.; Luis, A.S.; Stephen, F. Aeolian/fluvial interactions and high-resolution sequence stratigraphy of a non-marine lowstand wedge: The Avilé Member of the Agrio Formation (Lower Cretaceous), central Neuquén Basin, Argentina. *Sedimentology* **2002**, *49*, 1001–1019.
14. Yang, J.P.; Cao, Y.C. Sedimentary characteristics of flood inundation Lake in the lower part of the fourth member of Shahejie formation of Eogene in the west of Huimin Depression. *J. China Univ. Pet. (Ed. Nat. Sci.)* **2002**, *6*, 17–20. (In Chinese with English abstract)
15. Lin, C.S. Sequence sedimentary filling structure and process response of sedimentary basins. *Acta Sedimentol. Sinica.* **2009**, *27*, 849–862. (In Chinese with English abstract)
16. Laurent, G.; Daniel, L.H.; Hans, M.B. High resolution facies analysis and sequence stratigraphy of the Siluro-Devonian succession of Al Kufrah basin (SE Libya). *J. Afr. Earth Sci.* **2012**, *76*, 8–26.
17. Mohammad, A.S. High resolution sequence stratigraphic analysis of the Late Miocene Abu Madi Formation, Northern Nile Delta Basin. *NRIAG J. Astron. Geophys.* **2015**, *4*, 298–306.
18. Song, L.C.; Liu, C.L.; Zhang, J.D.; Qu, H.J. High-Resolution Sequence Stratigraphy of Shallow Lacustrine Delta Front: The Second Member of Sangonghe Formation, Central Junggar Basin. *Acta Geol. Sin. (Engl. Ed.)* **2015**, *89*, 314–315.
19. Lucas, V.V.; dos Santos Scherer, C.M. Facies architecture and high resolution sequence stratigraphy of an aeolian, fluvial and shallow marine system in the Pennsylvanian Piauí Formation, Parnaíba Basin, Brazil. *J. South Am. Earth Sci.* **2017**, *76*, 238–256.
20. Sapana, J.; Biplab, B.; Snehasis, C. High resolution sequence stratigraphy of Middle Eocene Hazad Member, Jambusar Broach Block, Cambay Basin, India. *Mar. Pet. Geol.* **2018**, *93*, 79–94.
21. Lisa, C.; Or, M.B.; Zvi, B.A. Late Quaternary lacustrine deposits of the Dead Sea basin: High resolution sequence stratigraphy from downhole logging data. *Quat. Sci. Rev.* **2019**, *210*, 175–189.
22. Carolyn, M.F.; Murray, K.G.; John, P.Z. High-resolution sequence stratigraphy of the Middle Triassic Sunset Prairie Formation, Western Canada Sedimentary Basin, north-eastern British Columbia. *Depos. Rec.* **2020**, *6*, 383–408.
23. Aimasgari, A.A.; Elsaadany, M.; Siddiqui, N.A. Geomorphological Geometries and High-Resolution Seismic Sequence Stratigraphy of Malay Basin's Fluvial Succession. *Appl. Sci.* **2021**, *11*, 5156. [CrossRef]
24. Liu, E.T.; Wang, H.; Li, Y. Sedimentary characteristics and tectonic setting of sublacustrine fans in a half-graben rift depression, Beibuwan Basin, South China Sea. *Mar. Pet. Geol.* **2014**, *52*, 9–21. [CrossRef]
25. Maravelis, A.; Boutelier, D.; Catuneanu, O.; Seymour, K.; Zelilidis, A. A review of tectonics and sedimentation in a forearc setting: Hellenic Thrace Basin, North Aegean Sea and Northern Greece. *Tectonophysics* **2016**, *674*, 1–19. [CrossRef]
26. Wei, W.; Lu, Y.; Xing, F.; Liu, Z.; Pan, L.; Algeo, T.J. Sedimentary facies associations and sequence stratigraphy of source and reservoir rocks of the lacustrine Eocene Niubao Formation (Lunpola Basin, central Tibet). *Mar. Pet. Geol.* **2017**, *86*, 1273–1290. [CrossRef]
27. Yue, Z.P.; Zeng, J.; Gao, Z.W. Sedimentary mechanism of "gypsum salt rock" layer of Kongdian formation Sha4 member in Huimin Depression—Taking the analysis of "gypsum salt rock" layer of well MS1 as an example. *Pet. Explor. Dev.* **2006**, *5*, 591–595. (In Chinese with English abstract)

28. Zhang, J.L.; Zhang, X. Composition and Provenance of Sandstones and Siltstones in Paleogene, Huimin Depression, Bohai Bay Basin, Eastern China. *J. China Univ. Geosci.* **2008**, *19*, 252–270. (In Chinese with English abstract)
29. Han, Z.Z.; Yang, R.C.; Fan, A.P. Remaining oil distribution in Ng 3 bottom water reservoir of Lin 2-6 fault-block in Huimin Depression and potential tapping in horizontal well. *Min. Sci. Technol. (China)* **2009**, *19*, 102–107. [CrossRef]
30. Zhang, J.L.; Li, D.Y.; Jiang, Z.Q. Diagenesis and reservoir quality of the fourth member sandstones of Shahejie formation in Huimin Depression, eastern China. *J. Cent. S. Univ. Technol.* **2010**, *17*, 169–179. (In Chinese with English abstract) [CrossRef]
31. Ni, J.; Guo, Y.; Wang, Z.; Liu, J.; Lin, Y.; Li, Y. Tectonics and mechanisms of uplift in the central uplift belt of the Huimin depression. *J. Earth Sci.* **2011**, *22*, 299–315. [CrossRef]
32. Li, Q.; Jiang, Z.X.; Liu, K.Y.; Zhang, C.M.; You, X.L. Factors controlling reservoir properties and hydrocarbon accumulation of lacustrine deep-water turbidites in the Huimin Depression, Bohai Bay Basin, East China. *Mar. Pet. Geol.* **2014**, *57*, 327–344. [CrossRef]
33. Pei, L.X.; Gang, W.Z.; Wang, D.M.; Xiong, M. Application of biomarkers to petroleum migration in the Linyi fault area, Huimin Depression, Bohai Bay Basin, China. *Can. J. Earth Sci.* **2017**, *54*, 311–321. (In Chinese) [CrossRef]
34. Li, C.; Luo, X.R.; Zhang, L.K.; Wang, B.; Guan, X.Y.; Luo, H.M.; Lei, Y.H. Overpressure Generation Mechanisms and Its Distribution in the Paleocene Shahejie Formation in the Linnan Depression, Huimin Depression, Eastern China. *Energies* **2019**, *12*, 3183. [CrossRef]
35. Wang, Q.C.; Chen, D.X.; Wang, F.W.; Li, J.H.; Liao, W.H.; Wang, Z.Y.; Xie, G.J.; Shi, X.B. Under pressure characteristics and origins in the deep strata of rift basins: A case study of the Huimin Depression, Bohai Bay Basin, China. *Geol. J.* **2020**, *55*, 4079–4096. [CrossRef]
36. Wang, S.B.; Zhong, J.H.; Chen, Z.P. Study on Cenozoic fault activity characteristics in Huimin Depression. *J. Geomech.* **2007**, *1*, 86–96. (In Chinese with English abstract)
37. Pirson, S.J. *Geiologic Well Log Analysis*; Gulf Publishing Company: Houston, TX, USA, 1970.
38. Tabanou, J.R.G.R.; Rouault, G.F. SP deconvolution and quantitative interpretation in shaly sands. In Proceedings of the 28th Annual Logging Symposium, London, UK, 29 June–2 July 1987; pp. 1–22.
39. Wang, S.M.; Liu, Z.J. Discussion on some problems of high resolution sequence stratigraphy in the study of continental stratigraphy. *J. Stratigr.* **2004**, *28*, 179–184. (In Chinese with English abstract)
40. Zhang, L.F.; Wu, C.J.; Su, Y. High resolution sequence stratigraphy of deep-water turbidite outcrop of Ross sandstone formation in Clare basin, Ireland. *Oil Gas Geol.* **2017**, *38*, 165–174. (In Chinese with English abstract)
41. He, Y.P.; Liu, Z.J.; Du, J.F. Identification of base level cycles in high resolution sequence stratigraphy. *Glob. Geol.* **2003**, *1*, 21–25. (In Chinese with English abstract)
42. Selly, R.C. *An Introduction to Sedimentology*; Academic Press Inc.: London, UK, 1976; pp. 208–209.
43. Li, Y.M.; Richard, A.S. Facies identification from well logs: A comparison of discriminant analysis and naïve Bayes classifier. *J. Pet. Sci. Eng.* **2006**, *53*, 149–157. [CrossRef]
44. Deng, H.W.; Wang, H.L.; Wang, J.F. Self-similarity of sequence stratigraphic composition and sequence sand and reservoir control—Taking delta turbidite fan system as an example. *Oil Gas Geol.* **2004**, *25*, 491–495. (In Chinese with English abstract)